Published online 17 February 2015 *Nucleic Acids Research, 2015, Vol. 43, No. 5* **2499–2512**
doi: 10.1093/nar/gkv109

2-Thiouracil deprived of thiocarbonyl function preferentially base pairs with guanine rather than adenine in RNA and DNA duplexes

Elzbieta Sochacka[1], Roman H. Szczepanowski[2], Marek Cypryk[3], Milena Sobczak[3], Magdalena Janicka[3], Karina Kraszewska[3], Paulina Bartos[1], Anna Chwialkowska[3] and Barbara Nawrot[3,*]

[1]Institute of Organic Chemistry, Technical University of Lodz, Zeromskiego 116, 90–924 Lodz, Poland, [2]International Institute of Molecular and Cell Biology, Ks. J. Trojdena 4, 02–109 Warsaw, Poland and [3]Centre of Molecular and Macromolecular Studies, Polish Academy of Sciences, Sienkiewicza 112, 90–363 Lodz, Poland

Received December 15, 2014; Revised January 30, 2015; Accepted February 02, 2015

ABSTRACT

2-Thiouracil-containing nucleosides are essential modified units of natural and synthetic nucleic acids. In particular, the 5-substituted-2-thiouridines (S2Us) present in tRNA play an important role in tuning the translation process through codon–anticodon interactions. The enhanced thermodynamic stability of S2U-containing RNA duplexes and the preferred S2U-A versus S2U-G base pairing are appreciated characteristics of S2U-modified molecular probes. Recently, we have demonstrated that 2-thiouridine (alone or within an RNA chain) is predominantly transformed under oxidative stress conditions to 4-pyrimidinone riboside (H2U) and not to uridine. Due to the important biological functions and various biotechnological applications for sulfur-containing nucleic acids, we compared the thermodynamic stabilities of duplexes containing desulfured products with those of 2-thiouracil-modified RNA and DNA duplexes. Differential scanning calorimetry experiments and theoretical calculations demonstrate that upon 2-thiouracil desulfuration to 4-pyrimidinone, the preferred base pairing of S2U with adenosine is lost, with preferred base pairing with guanosine observed instead. Therefore, biological processes and *in vitro* assays in which oxidative desulfuration of 2-thiouracil-containing components occurs may be altered. Moreover, we propose that the H2U-G base pair is a suitable model for investigation of the preferred recognition of 3′-G-ending versus A-ending codons by tRNA wobble nucleosides, which may adopt a 4-pyrimidinone-type structural motif.

INTRODUCTION

Sulfur-containing nucleosides constitute a class of nucleosides present in natural nucleic acids (http://rna-mdb.cas.albany.edu; http://modomics.genesilico.pl) (1,2). Among these molecules is a subset of 5-substituted derivatives of 2-thiouridine (S2U) (Figure 1), which are located in the first anticodon position in transfer RNAs (tRNAs) specific for lysine, glutamic acid and glutamine. 2-Thiouridines greatly contribute to translational regulation through codon–anticodon interactions (3–9). Moreover, the sulfur-modified units serve as recognition elements for cognate aminoacyl tRNA synthetases (aa-RS) (10,11) and are used together with other modifications by the innate immune system to distinguish between self and pathogen RNAs (12–14). Furthermore, the thiocarbonyl function of S2U-containing human $tRNA^{Lys3}$ is involved in the formation of the initial complex with HIV-1 RNA as a prerequisite for viral RNA reverse transcription (15). Notably, 5-methyl-2-thiouridine (or 2-thioribothymidine) is also located in the TΨC loop of tRNAs of hyperthermophilic species such as *Thermus thermophilus* (16,17) and *Pyrococcus furiosus* (18). This nucleoside is thought to enhance the stability of the tertiary structure of tRNA at elevated temperatures.

RNA duplexes containing S2U-A base pairs are thermodynamically more stable than those with U-A base pairs due to a preferential S2U C3′-*endo* sugar ring pucker, which improves base stacking in RNA chains and enhances an overall A-type RNA duplex helical structure (19–26). Furthermore, 2-thiouridines preferentially hybridize with adenosines, whereas wobble pairing with guanosine residues is restricted due to less effective hydrogen bonding between the N(1)H donor of guanine and the sulfur acceptor in 2-thiouracil.

The enhanced thermodynamic stability of S2U-containing RNA duplexes and the preference for S2U-A

*To whom correspondence should be addressed. Tel: +48 42 6803248; Fax: +48 6815483; Email: bnawrot@cbmm.lodz.pl

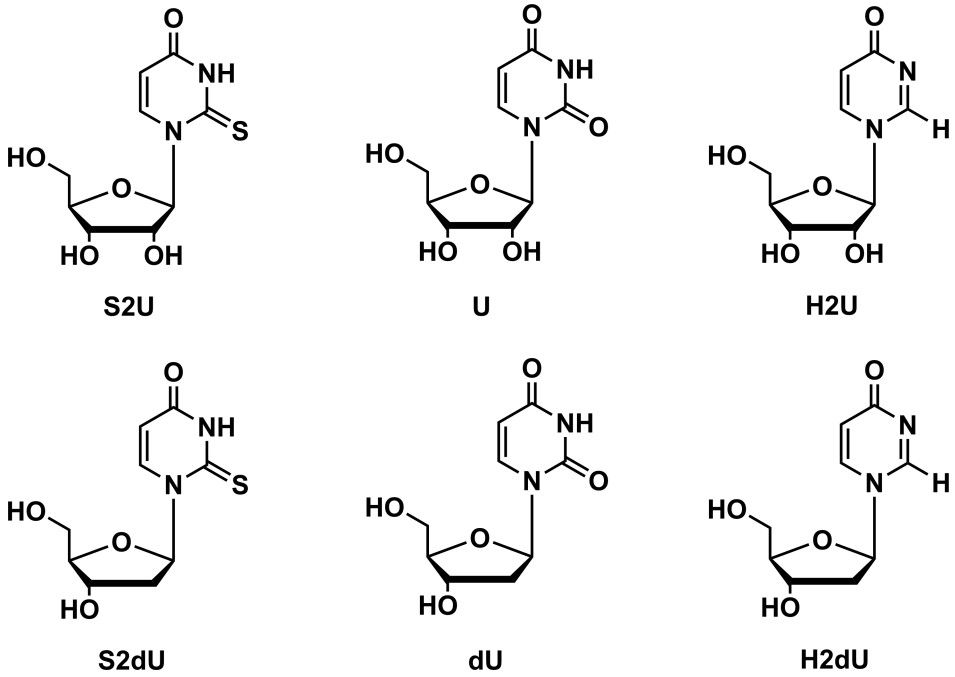

Figure 1. The structures of modified nucleosides used in the present studies: 2-thiouridine (S2U), uridine (U), 4-pyrimidinone riboside (H2U), 2′-deoxy-2-thiouridine (S2dU), 2′-deoxyuridine (dU), 4-pyrimidinone 2′-deoxyriboside (H2dU).

versus S2U-G base pairing are appreciated characteristics of S2U-containing molecular probes used in nucleic acids biology and medicinal chemistry. For example, S2U alone or in combination with 2′-*O*-sugar modifications built into RNA chains increases the silencing activity of short interfering RNAs, rendering these modified duplexes promising tools for RNAi therapy (27–30). RNA probes containing 2′-*O*-methylated 2-thiouridine (immobilized on glass) effectively discriminate complements with complementary A versus mismatched G residues (31). Even more potent discrimination is achieved by the replacement of 2′-*O*-methylribose with an Locked Nucleic Acid (LNA) type bicyclic sugar analog (32). 2-Thio-5-methyluridine in combination with 2′-*O*-[2-(methoxy)ethyl] sugar modifications improves the thermodynamic stability and nuclease resistance of DNA/RNA heteroduplexes composed of modified DNA and complementary RNA (33). Moreover, 2-thiouridine-5′-*O*-di- and triphosphates and their analogs were found to be potent and selective agonists of the P2Y2 and P2Y14 receptors (34–36), whereas S2U-RNAs were used in Structure-Activity Relationship (SAR) studies of Toll-like receptors (12,13) and as suppressors of the interferon-inducible protein kinase PKR (14).

Additionally, 2-thio-2′-deoxyuridine (S2dU) and 2-thiothymidine (S2T)-labeled DNA oligomers have been widely used in molecular biology, biochemistry and biotechnology. In contrast to S2U, in S2dU and S2T, the sugar rings preferentially adopt C2′-*endo* puckering, which is present in the parent dU and T nucleosides (21,37). The strength of S2T-A base pairing is virtually identical to that in a T-A system (38–40). Studies on the fidelity of DNA replication conducted using an S2T-modified template confirmed the discrimination between complements containing A and those in which complementary A was substituted with a mismatched G residue (41). This result was also confirmed by hybridization studies demonstrating higher stability of the S2T-dA base pair compared with the S2T-dG base pair in DNA duplexes. Additionally, 2-thiothymidine 5′-*O*-triphosphate, which was evaluated as a substrate for the Klenow fragment of DNA Pol I, was 2.2-fold more efficient than TTP (41) and was useful in six-letter genetic alphabet PCR amplification due to increased fidelity of non-canonical *iso*-dC-*iso*-dG base pairing compared with S2T-*iso*-dG base pairing (42). In self-avoiding molecular recognition systems, S2T allows the discrimination between duplexes with strong S2T-dA base pairs and those with an unfavorable S2T-2-aminopurine nucleoside pattern (43).

Because of the important biological functions and various biotechnological applications of sulfur-modified nucleosides and oligonucleotides that contain them, determination of their stability under *in vitro* oxidative stress conditions and the influence of their possible oxidative lesions on the structure and function of S2U-containing nucleic acids are of significant importance. We have previously shown that under conditions mimicking oxidative stress in a cell (aqueous H_2O_2), S2U is effectively transformed into a mixture of uridine (U) and 4-pyrimidinone riboside (H2U) (Figure 1), and the product ratio is pH (44) and concentration dependent (E. Sochacka *et al.*, in preparation). Similarly, treatment of S2U-containing RNA with 100 mM H_2O_2 (in either water or a buffered solution at pH 7.5) produced corresponding desulfured products, and also in this case, the H2U-containing RNA was a major product (45). Notably, the hydrogen bonding donor/acceptor pattern in 4-pyrimidinone differs from that in uracil/2-

thiouracil. Moreover, we demonstrated that the sugar ring in H2U predominantly adopts the C2′-*endo* conformation (typical for B-type DNA), which is substantially different from the C3′-*endo* conformation preferentially adopted by S2U (46). Undoubtedly, these two structural differences affect the Watson–Crick type interactions of H2U with adenine and the wobble interactions with guanine. Therefore, one may assume that the S2U→H2U transformation alters the thermal stability of RNA duplexes (45) and possibly their S2T/S2dU DNA congeners (47). This replacement may result in significant consequences for biological processes in which 2-thiouracil-containing nucleic acids are involved (48). Of note, anticodon-specific endonucleases are also known to induce tRNA cleavage, which is a conserved response to oxidative stress in numerous eukaryotic species ranging from *Saccharomyces cerevisiae* and *Arabidopsis* to humans (49).

To study the S2U→H2U transformation effects, we prepared a series of RNA and DNA duplexes containing uracil, 2-thiouracil or 4-pyrimidinone interacting with a complementary adenine or guanine residue (Table 1). Model-independent differential scanning calorimetry (DSC) was used to determine the thermodynamic stability of the duplexes. Moreover, we performed quantum chemical Discrete Fourier Transform (DFT) calculations and molecular mechanics modeling to assess the energies of base pairing in isolated base pairs and in pairs of nucleotides within RNA and DNA duplexes.

MATERIALS AND METHODS

Synthesis and purification of model oligonucleotides

The synthesis of non-modified DNA and RNA oligonucleotides listed in Supplementary Table S1 was done on a Gene World DNA synthesizer at the 0.2 μm scale using the phosphoramidite approach and the standard protocol, except for the synthesis of oligonucleotides containing 2-thiouracil and 4-pyrimidinone nucleobases (Figure 1), for which modified synthetic procedures described below were applied.

Synthesis of RNA oligomers

Synthesis of 14-mer RNAs containing S2U and H2U (Supplementary Table S1) was done using commercial (Glen Research and ChemGene) ultra-mild TBDMS ribonucleoside phosphoramidites of suitably protected nucleosides U, C, A and G, and the S2U and H2U monomers, obtained in house according to the previously described procedures (50,51). The coupling time for the modified units was prolonged to 15 min. The P(III)→P(V) oxidation step in the synthesis of the S2U-oligonucleotide was performed with 0.25 M solution of tBuOOH in CH_3CN for 5 min, while for the H2U-oligomer the standard iodine oxidation was applied.

The RNA oligonucleotide containing 2-thiouridine was deprotected and cleaved from the solid support by treatment with a mixture of concentrated (conc.) aqueous ammonia and ethanol (3:1) for 16 h at 37°C. The solution was evaporated under reduced pressure (Speed Vac). The S2U-RNA was purified either by RP-HPLC in a routine TEAB/Acetonitrile (pH 7.5) solvent system or by IE-HPLC by elution with a linear gradient of NaBr (50–650 mM) in sterile 20 mM Na_2HPO_4–NaH_2PO_4 buffer solution (pH 7.5), containing EDTA (50 μM) and 10% acetonitrile. The obtained eluates were desalted on C18 SepPak cartridges (Waters).

The oligomer containing 4-pyrimidinone nucleoside (H2U), because of its instability in aqueous alkali, was cleaved from the solid support and deprotected by the treatment with 0.05 M K_2CO_3 in anhydrous MeOH for 16 h at 30°C. The solution was neutralized with diluted acetic acid and evaporated. The resultant dry pellets were treated with the 1:1 (v/v) mixture of triethylamine tris(hydrofluoride) and of dry dimethylformamide (DMF) (120 μl) for 16 h at 25°C. The reactions were quenched by addition of the same volume of isopropyl trimethylsilyl ether, shaken until a precipitate appeared and centrifuged. The pellets were washed three times with diethyl ether and then dried *in vacuo*.

The fully deprotected RNA oligomers were purified by IE-HPLC in a gradient of buffer B (600 mM $NaClO_4$, 10% CH_3CN, 50 mM Tris-HCl, 50 μM EDTA, pH 7.6) in buffer A (10 mM $NaClO_4$, 10% CH_3CN, 50 mM Tris-HCl, 50 μM EDTA, pH 7.6) and desalted on C18 SepPak cartridges (Waters). The molecular mass of all synthesized oligomers was confirmed by MALDI-TOF mass spectrometry (Supplementary Table S1), and purity by polyacrylamide gel electrophoresis (PAGE) analysis (not shown).

Synthesis of DNA oligomers

Synthesis of 14-mer DNAs containing S2dU and H2dU (Supplementary Table S1) was done using commercial nucleoside phosphoramidites of suitably protected nucleosides T, dC, dA and dG, and the S2dU and H2dU monomers, obtained in house according to previously described procedures (46). For the synthesis of H2dU-oligonucleotide, the monomers with 'mild' Pac protecting groups (Glen Research) were used. Coupling of modified monomers was allowed to proceed for 220 s. The P(III)→P(V) oxidation step in the synthesis of the S2dU-oligonucleotide was performed with 0.25 M solution of tBuOOH in CH_3CN for 5 min, while for H2dU-oligomer, standard iodine oxidation was applied. The DNA oligonucleotide containing 2-thio-2′-deoxyuridine was cleaved from the solid support by treatment with a mixture of conc. 30% aqueous ammonia and ethanol (3:1) for 4 h at 55°C and deprotected by the two-step procedure (DMT-on, DMT-off) (52). The solution was evaporated under reduced pressure (Speed Vac) and loaded on the RP semipreparative column (Hamilton PRP-1 (7 mm × 305 mm, C-18, 10 μm), and eluted with 0.1 M ammonium acetate (buffer A), and 0.1 M ammonium acetate and 40% acetonitrile (buffer B) with the elution of 3 ml/min in the following program: DMT-on 0–100% buffer B in 30 min, and for DMT-off 0–100% buffer B in 15 min. The obtained eluates were desalted on C18 SepPak cartridges (Waters). The oligomer containing 4-pyrimidinone nucleoside (H2dU), because of its instability in aqueous alkali, was cleaved from the solid support and deprotected by the treatment with 1 ml of 0.05 M K_2CO_3 in anhydrous MeOH for 16 h at 30°C. The solution was neutralized by diluted acetic acid and evaporated. The fully deprotected oligomer was purified by AE-HPLC on semipreparative MonoQ col-

Table 1. The sequences of the investigated RNA (1–6) and DNA (7–14) duplexes, their abbreviated names (in bold) and an indication of a Watson–Crick (WC) or wobble (WB) pairing mode

No.	Duplex sequence	Name	Pairing mode#
1	5′-CGGCU **U** UUAACCGA-3′ 3′-GCCGA **A** AAUUGGCU-5′	**U-A**	WC
2	5′-CGGCU **S2U** UUAACCGA-3′ 3′-GCCGA **A** AAUUGGCU-5′	**S-A**	WC
3	5′-CGGCU **H2U** UUAACCGA-3′ 3′-GCCGA **A** AAUUGGCU-5′	**H-A**	WC
4	5′-CGGCU **U** UUAACCGA-3′ 3′-GCCGA **G** AAUUGGCU-5′	**U-G**	WB
5	5′-CGGCU **S2U** UUAACCGA-3′ 3′-GCCGA **G** AAUUGGCU-5′	**S-G**	WB
6	5′-CGGCU **H2U** UUAACCGA-3′ 3′-GCCGA **G** AAUUGGCU-5′	**H-G**	WB*
7	5′-d(CGGCT **T** TTAACCGA)-3′ 3′-d(GCCGA **A** AATTGGCT)-5′	**T-dA**	WC
8	5′-d(CGGCT **dU** TTAACCGA)-3′ 3′-d(GCCGA **A** AATTGGCT)-5′	**dU-dA**	WC
9	5′-d(CGGCT **S2dU** TTAACCGA)-3′ 3′-d(GCCGA **A** AATTGGCT)-5′	**dS-dA**	WC
10	5′-d(CGGCT **H2dU** TTAACCGA)-3′ 3′-d(GCCGA **A** AATTGGCT)-5′	**dH-dA**	WC
11	5′-d(CGGCT **T** TTAACCGA)-3′ 3′-d(GCCGA **G** AATTGGCT)-5′	**T-dG**	WB
12	5′-d(CGGCT **dU** TTAACCGA)-3′ 3′-d(GCCGA **G** AATTGGCT)-5′	**dU-dG**	WB
13	5′-d(CGGCT **S2dU** TTAACCGA)-3′ 3′-d(GCCGA **G** AATTGGCT)-5′	**dS-dG**	WB
14	5′-d(CGGCT **H2dU** TTAACCGA)-3′ 3′-d(GCCGA **G** AATTGGCT)-5′	**dH-dG**	WB*

WB* is a wobble H2U-G-type base pair shown in Figure 7.

umn (4.6 mm × 100 mm, PE), elution of 1 ml/min; in the gradient of buffer B (600 mM $NaClO_4$ and 10% acetonitrile + 50 mM Tris-HCl + 50 μM EDTA, pH7.6) in buffer A (10 mM $NaClO_4$, 10% acetonitrile, 50 mM Tris-HCl, 50 μM EDTA, pH 7.6) in the following scheme: time 0–5 min: A90%, B10%; 5–45 min: B10%-60%; 45–48 min: B60%-100%. The obtained eluates were desalted on C18 SepPak cartridges (Waters). The molecular mass of all synthesized oligonucleotides was confirmed by MALDI-TOF mass spectrometry (Supplementary Table S1), and purity by PAGE analysis (not shown).

Annealing of duplexes

DNA and RNA concentrations of aqueous stock solutions were determined from their absorbance at 260 nm using a Cintra 10e Spectrometer (GBC Scientific Equipment Ltd, Australia). Single strand extinction coefficients were calculated according to a nearest-neighbour model (53,54). Annealing of RNA and DNA duplexes (Table 1) was performed in deionized water by heating the mixture of RNA or DNA oligonucleotides and their complementary strands (1:1 molar mixture) at 95°C for 5 min, followed by slow cooling down to a room temperature (over 2 h). Samples were concentrated on the Speed Vac. The duplexes prepared for these studies are listed in Table 1.

DSC melting measurements

DSC measurements were performed using a MicroCal VP-DSC microcalorimeter, equipped with 0.514 ml cells. Dry samples of annealed duplexes were diluted with a 10 mM phosphate buffer containing 50 mM NaCl to the final concentrations 20 μM and degassed for 10 min at 18°C. External pressure of 30 psi was applied to the sample and reference cells. Three independent dilutions of each duplex were studied. The VP-DSC was run without feedback, within temperature range 10–95°C (up scans only), at a heating rate 40°C/h. A 10-min equilibration time at 10°C was used before and between scans. Three-to-ten buffer–

buffer scans were performed initially to establish a 'thermal history' of the instrument, to obtain baseline and confirm reproducibility of the measurements. Then, the buffer in the sample cell was replaced by the oligonucleotide duplex solution and several scans were collected. DSC data were analyzed using ORIGIN software from MicroCal. For both, the buffer and the RNA sample, the second scans were used (all scans after the first, except few cases discussed later, were indistinguishable). Data were corrected for instrument baselines and normalized for the scan rate and the nucleic acid concentration. A cubic baseline was fitted to each profile and subtracted. To avoid controversy about the proper fitting model (which is quite common, especially for short oligonucleotide duplexes) (55) and to make the calculations model independent, enthalpies (ΔH_{cal}) and entropies (ΔS_{cal}) of duplex formation were calculated from the areas under the experimental ΔCp versus T and derived from $\Delta Cp/T$ versus T curves, respectively, while free energy (ΔG_{25}) values were calculated according to the standard equation $\Delta G_{25} = \Delta H - (298.15)\Delta S$ (56). The results of three independent experiments were averaged. In some cases, in subsequent measurements of the same duplex, variation of pre- and post-unfolding baseline was observed. This was reflected in a higher standard deviation (SD). The errors were calculated as $\pm$SD of the three independent measurements of each duplex.

Circular dichroism measurements

Samples of the RNA and DNA duplexes were prepared at 2 μM concentration in a 10-mM phosphate buffer, pH 7.0, containing 50 mM NaCl. The spectra were recorded at a room temperature on a Jobin Yvon CD6 Dichrograf. Measurements were made in optically matched 0.5 cm pathlength quartz cuvettes of 1 ml capacity, 2 nm bandwidth and 1–2 s integration time. Each spectrum was smoothed with 9- and 15-point algorithm (included in the manufacturer's software, version 2.2.1) after averaging of at least three scans.

Computational methods

All quantum mechanical calculations were performed with the Gaussian 09 suite of programs (57). Geometries of the base pair model systems were optimized using the hybrid B3LYP functional with 6–31G(d) basis set in the gas and water phase. Methyl substituents were used in place of ribose moieties. All the stationary points have been identified to correspond to the stable minima by frequency calculations. Vibrational analysis also provided thermal enthalpy and free energy corrections to 298 K. More accurate electronic energies were obtained using the long-range and dispersion corrected ωB97XD functional with the 6–311++G(3df,2p) basis set for B3LYP/6–31G(d) geometries. This level of theory gives reasonable accuracy in thermochemical calculations (mean absolute error in test calculations was of ca. 2 kcal/mol) (58). basis set superposition error (BSSE) error was neglected since it was found to be unimportant at this level of theory (test calculations at B3LYP/6–311+G(2d,p)//B3LYP/6–31G(d) showed BSSE of 0.3 kcal/mol and 0.4 kcal/mol for H2U-A and H2U-G pairs, respectively). Since the 6–311++G(3df,2p) basis set is larger than 6–311+G(2d,p), the BSSE is expected to be even smaller. Calculations in water solution were performed assuming polarizable conductor calculation model (CPCM) with radii = UFF option. Geometry optimizations and thermochemical corrections in solution were performed at the B3LYP/6–31+G(d) level and final energies were calculated at CPCM/ωB97XD/6–311++G(3df,2p).

The nine base pairs (bp) RNA duplexes were constructed using the HyperChem polynucleotide builder and optimized with Amber96 force field (59) using the Hyperchem 8 software (HyperChem(TM) Professional 8.0.10). For the detailed procedure see the Supplementary Information. The model RNAs of the following sequence 5′-GCU**U***UUAAC-3′, where U* is either uridine or 4-pyrimidinone riboside, together with the complementary 3′-CGA**Y**AAUUC-5′ strand, where Y is A or G, were created to mimic the base pair interactions in the discussed original RNA duplexes 1, 3, 4 and 6, respectively (Table 1). The fragments of model isosequential DNA duplexes containing HdU-dA and HdU-dG base pairs are shown in the Supplementary Information (Supplementary Figure S3).

RESULTS

Preparation of RNA and DNA duplexes

All of the RNA and DNA oligonucleotides containing modified units (for sequences, see Supplementary Table S1) were synthesized according to routine phosphoramidite methodology using in-house synthesized phosphoramidite monomers of the modified nucleosides S2U, S2dU, dU, H2U and H2dU (Figure 1) (45,46). A prolonged coupling time and modified oxidation step (0.25 M solution of tBuOOH in CH_3CN for 5 min) were used for the synthesis of RNA and DNA oligonucleotides containing S2U/S2dU units. A prolonged coupling time was also used for the synthesis of RNA and DNA oligomers modified with 4-pyrimidinone nucleosides. The S2U/S2dU-oligonucleotides were deprotected and cleaved from a solid support by treatment with a mixture of conc. aqueous ammonia and ethanol (3:1) due to the instability of 4-pyrimidinone nucleosides in aqueous alkali, and H2U/H2dU-oligomers were cleaved from a solid support and deprotected by treatment with 0.05 M K_2CO_3 in anhydrous MeOH. Following neutralization and solvent evaporation, the tBDMS protecting groups were removed from the RNA oligomers using Et_3Nx3HF/DMF, followed by quenching with isopropyl trimethylsilyl ether. The crude RNA and DNA products were subjected to IE-HPLC and desalted using C18 Sep-Pak cartridges. The sequences of the obtained oligonucleotides and their mass spectrometric characteristics are provided in the Supplementary Information (Supplementary Table S1).

DSC analysis of the RNA duplexes

*Analysis of the thermodynamic stability of the **H-A**, **S-A** and **U-A** RNA duplexes.* DSC experiments were performed for a series of six RNA duplexes, **1–6** (summarized in Table 1), containing U, S2U or H2U interacting with an A or G in the complementary strand. The recorded DSC profiles of the thermal dissociation of the RNA duplexes are shown

in Figure 2A, and the melting temperatures, T_m, and other thermodynamic parameters of the transitions are summarized in Table 2.

Here, using model-independent DSC measurements (60), we obtained accurate T_m, ΔH, ΔS and ΔG parameters for the dissociation transitions (Table 2). These results demonstrate that the most stable duplex is **S-A** followed by **U-A**, whereas the least stable duplex is **H-A** (containing the H2U-A pair). The T_m of 53°C for **H-A** is 11.2°C and 7.2°C lower than that for **S-A** and **U-A**, respectively. The ΔG_{25} value (the absolute value) for **H-A** is the smallest of the three RNA duplexes. The DSC transition profile of the **H-A** duplex (Figure 2A) contains an additional shoulder at a T_m of ∼36°C, which can be attributed to 'pre-melting' of the underlined 5 bp range in 5′-CGGCUH2UUUAACCGA-3′/3′-GCCGAAAAUUGGCU-5′. Moreover, the results obtained from DSC analysis unequivocally confirm that the 2-thiouridine within the **S-A** RNA duplex greatly increases the specificity of the interactions with adenine compared with uridine (within **U-A**), with a T_m value that is higher by 4°C and a ΔG_{25} value that is lower by 1.4 kcal/mol.

*Analysis of the thermodynamic stability of the **H-G**, **S-G** and **U-G** RNA duplexes.* The **U-G** and **S-G** duplexes, which contain U and S2U residues that interact with a G residue in the complementary strand, are thermally less stable than the corresponding duplexes containing a complementary A residue (Table 2 and Figure 2A), and this characteristic has been well documented for wobble base pairing, particularly in the context of codon–anticodon interactions. Although the difference in T_m (ΔT_m) between **U-A** and **U-G** is ∼3°C, the substantially preferred hybridization of S2U with A versus G is demonstrated by the ΔT_m of ∼10.0°C found for **S-A** versus **S-G**.

Additional results are related to the interactions between S2U, U and H2U and the guanine nucleoside. S2U destabilizes **S-G** to a greater extent than U destabilizes **U-G** (T_m = 54.2 versus 57.1°C). Interestingly, when S2U was replaced with H2U, the ΔT_m between the resultant **H-G** and parent **S-G** became negligible (−0.4°C), although $\Delta\Delta G_{25} = 1.5$ kcal/mol was found. Moreover, the ΔT_m between **H-G** and **U-G** was small (2.5°C, $\Delta\Delta G_{25}$ = 4.1 kcal/mol); thus, the degree of discrimination by S2U, U and H2U of the guanine nucleoside is much smaller than that for the series of duplexes containing a complementary A residue.

DSC analysis of the DNA duplexes

To study the effects of the S2dU to H2dU conversion on the thermal stability of the respective DNA duplexes, we used DNA duplexes isosequential to those in the RNA series and introduced the modified 2′-deoxyribonucleosides S2dU, dU and H2dU (shown in Figure 1) into the DNA strands. The T_m values and thermodynamic parameters of the dissociation transition for duplexes with complementary 2′-deoxyadenosine (duplexes **7–10**, Table 1) and 2′-deoxyguanosine (duplexes **11–14**, Table 1) are provided in Table 3, and the respective dissociation profiles are shown in Figure 2B.

*Analysis of the thermodynamic stability of the **T-dA**, **dU-dA**, **dS-dA** and **dH-dA** duplexes.* Analysis of the DSC melting results for duplexes **7–10** indicates that the most stable duplex is the canonical **T-dA** duplex, whereas for **dU-dA** (containing the parent thymidine residue lacking the methyl group at carbon atom C5), the T_m was lower by 1.9°C ($\Delta\Delta G$ = −1.1 kcal/mol). Introduction of a sulfur atom to the uracil moiety in dU resulted in a **dS-dA** duplex of only slightly higher T_m (ΔT_m = 0.8°C; the ΔG_{25} values were virtually equal). Replacement of S2dU with H2dU produced a **dH-dA** (**10**) duplex with a T_m value that was lower by ∼13°C compared with the T_m values for **dU-dA** and **dS-dA**. In this case, the ΔH and ΔG_{25} values of the dsDNA→ssDNA transition dramatically increased and were the least negative of all of the evaluated DNA duplexes (**7–14**). An additional transition at a T_m of ∼24°C was also observed in the DSC profile, which, as observed for the **H-A** duplex, may be attributed to dissociation of the 5 bp segment of the **dH-dA** duplex (underlined, 5′-d(CGGCU)H2dUd(UUAACCGA)-3′/3′-d(GCCGAAAAUUGGCU)-5′).

*Analysis of the thermodynamic stability of the **T-dG**, **dU-dG**, **dS-dG** and **dH-dG** duplexes.* In the DNA duplex series containing modified pyrimidine nucleosides complementary to dG (**11–14**, Table 1), **dH-dG** (**14**) was thermally more stable than the remaining **T-dG**, **dU-dG** and **dS-dG** duplexes ($\Delta\Delta T_m$ of 3–4°C, Table 3). Interestingly, the ΔG_{25} values for **dS-dG** and **dH-dG** were similar (ΔG_{25} = −7.4 ± 1.2 and −8.6 ± 0.1 kcal/mol, respectively) but were remarkably lower than that for **dH-dA** (ΔG = −5.5 ± 0.4 kcal/mol).

Circular dichroism analysis of the helical structure of the RNA and DNA duplexes

RNA duplexes **1–6** and DNA duplexes **7–14** were analyzed using circular dichroism (CD) spectroscopy. As shown in the CD spectra (Figure 3A and B), all RNA duplexes adopted an A-type overall conformation (a positive band at λ_{max} of ∼265 nm and a negative band at λ_{max} of 210 nm) (61). Minor differences, such as a slight increase in the intensity of the positive band at λ_{max} of 265 nm of the **S2U-A** and **S2U-G** duplexes (Figure 3A and B), were noted, which is most likely due to their improved π–π base stacking (62). The H2U residue complementary to A or G did not significantly alter the global RNA helical structure of **H-A** and **H-G**. In the CD spectra for DNA duplexes **7–14,** typical positive bands at approximately λ_{max} of 220 and 272 nm and negative bands at λ_{max} of 245 nm were present (63), although there were some differences in the CD shape of the B-type helical structure of **dS-dA** and **dS-dG** (the green profiles in Figure 3C and D). For both duplexes, the bands at λ_{max} of 272 nm and the isoelliptic point at 257 nm were blue shifted, whereas for **dS-dG**, the isoelliptic point at 223 nm was red shifted. For **dH-dG** (the red profile in Figure 3D) the long-wave positive CD band at 272 nm was significantly decreased compared with the CD profiles of **T-dG** and **dU-dG**.

Theoretical calculations

Base pair models. Quantum chemical DFT calculations of the free base pairs were performed to determine the struc-

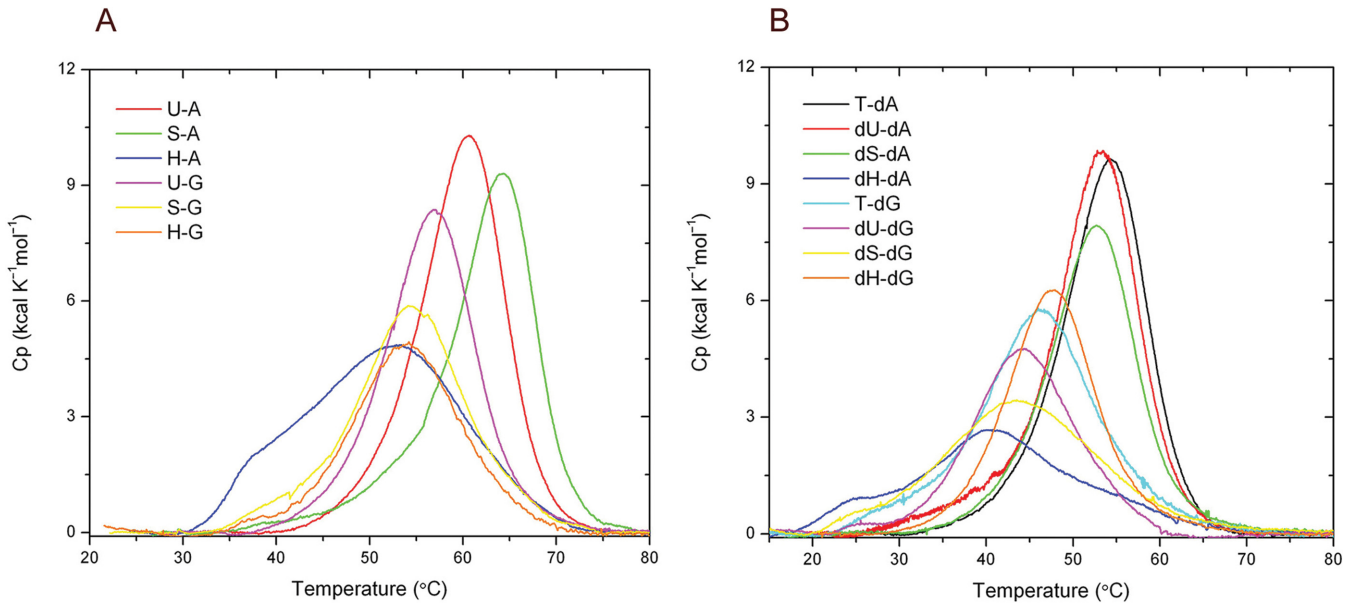

Figure 2. The DSC profiles of the thermal dissociation of the RNA duplexes (**A**) **U-A** (**1**), **S-A** (**2**), **H-A** (**3**), **U-G** (**4**), **S-G** (**5**), **H-G** (**6**) and the DNA duplexes (**B**) **T-dA** (**7**), **dU-dA** (**8**), **dS-dA** (**9**), **dH-dA** (**10**), **T-dG** (**11**), **dU-dG** (**12**), **dS-dG** (**13**), **dH-dG** (**14**). The sequences of duplexes are listed in Table 1.

Table 2. Thermodynamic parameters of the dissociation of the RNA duplexes determined by DSC

No.	Name	T_m [°C] for duplex [20 μM]	-ΔH ± SD [kcal/mol]	-ΔS_{cal} ± SD [cal/K mol]	-ΔG_{25} for duplex formation [kcal/mol]
1	**U-A**	60.3 ± 0.3	111.6 ± 5.6	335.8 ± 16.6	15.1 ± 0.8
2	**S-A**	64.3 ± 0.1	116.4 ± 2.8	348.0 ± 8.6	16.5 ± 0.4
3	**H-A**	53.1 ± 0.4	96.0 ± 8.2	296.1 ± 25.2	11.0 ± 1.0
4	**U-G**	57.1 ± 0.3	106.8 ± 2.6	324.2 ± 7.5	13.7 ± 0.5
5	**S-G**	54.2 ± 0.2	91.0 ± 0.5	278.0 ± 1.4	11.1 ± 0.1
6	**H-G**	54.6 ± 0.3	76.1 ± 3.7	231.6 ± 10.7	9.6 ± 0.6

All values are derived as averages of three independent measurements.

Table 3. Thermodynamic parameters of the dissociation transitions of the DNA duplexes determined by DSC methodology

No.	Name	T_m [°C] for duplex [20 μM]	-ΔH ± SD [kcal/mol]	-ΔS_{cal} ± SD [cal/K mol]	-ΔG_{25} for duplex formation [kcal/mol]
7	**T-dA**	54.6 ± 0.4	118.0 ± 2.9	361.5 ± 9.2	14.2 ± 0.3
8	**dU-dA**	52.7 ± 0.0	113.6 ± 9.5	349.8 ± 29.5	13.1 ± 1.0
9	**dS-dA**	53.5 ± 0.7	103.8 ± 5.1	318.5 ± 16.7	12.3 ± 0.8
10	**dH-dA**	40.3 ± 0.3	61.4 ± 0.8	194.8 ± 2.6	5.5 ± 0.4
11	**T-dG**	45.2 ± 0.7	96.8 ± 2.9	304.8 ± 9.6	9.3 ± 0.3
12	**dU-dG**	44.3 ± 0.2	87.1 ± 24.9	271.4 ± 79.5	9.1 ± 2.2
13	**dS-dG**	44.5 ± 0.9	77.1 ± 5.7	242.9 ± 16.7	7.4 ± 1.2
14	**dH-dG**	48.5 ± 1.1	84.2 ± 0.9	263.2 ± 3.3	8.6 ± 0.1

All values are derived as averages of three independent measurements.

tures of the hydrogen-bonded complexes and the bonding enthalpies between nucleobases of interest. In all of the evaluated base models, the ribose residue of the parent nucleoside was replaced with a methyl group. Atomic charges for the 4-pyrimidinone fragment of H2U were calculated at the B3LYP/6–311+G(2d,p) level using the ESP (Merz-Kollman) scheme as described in the Supplementary Information (see Supplementary Figure S1). The enthalpies of bonding for the classical base pairs have been previously calculated at various levels of theory (64–67). Structures and bonding enthalpies for the base pairs under consideration (Figure 4) demonstrate that the 4-pyrimidinone–adenine that base pairs with a single O(4)...HN(6) hydrogen bond is weak and does not reach the energy minimum upon optimization. Rather, optimization in water produces a wobble-like base pair with binding enthalpy $\Delta H = -4.8$ kcal/mol with a weak stabilizing interaction between the H-C(2) hydrogen of the 4-pyrimidinone moiety and the endocyclic N(1) nitrogen atom of adenine (Figure 4C) (68,69). For the remaining two base pairs of adenine (U-A and S2U-A, Figure 4A and B), the binding enthalpies are similar or identical, with $\Delta H = -9.1$ kcal/mol under the evaluated conditions (aqueous solution).

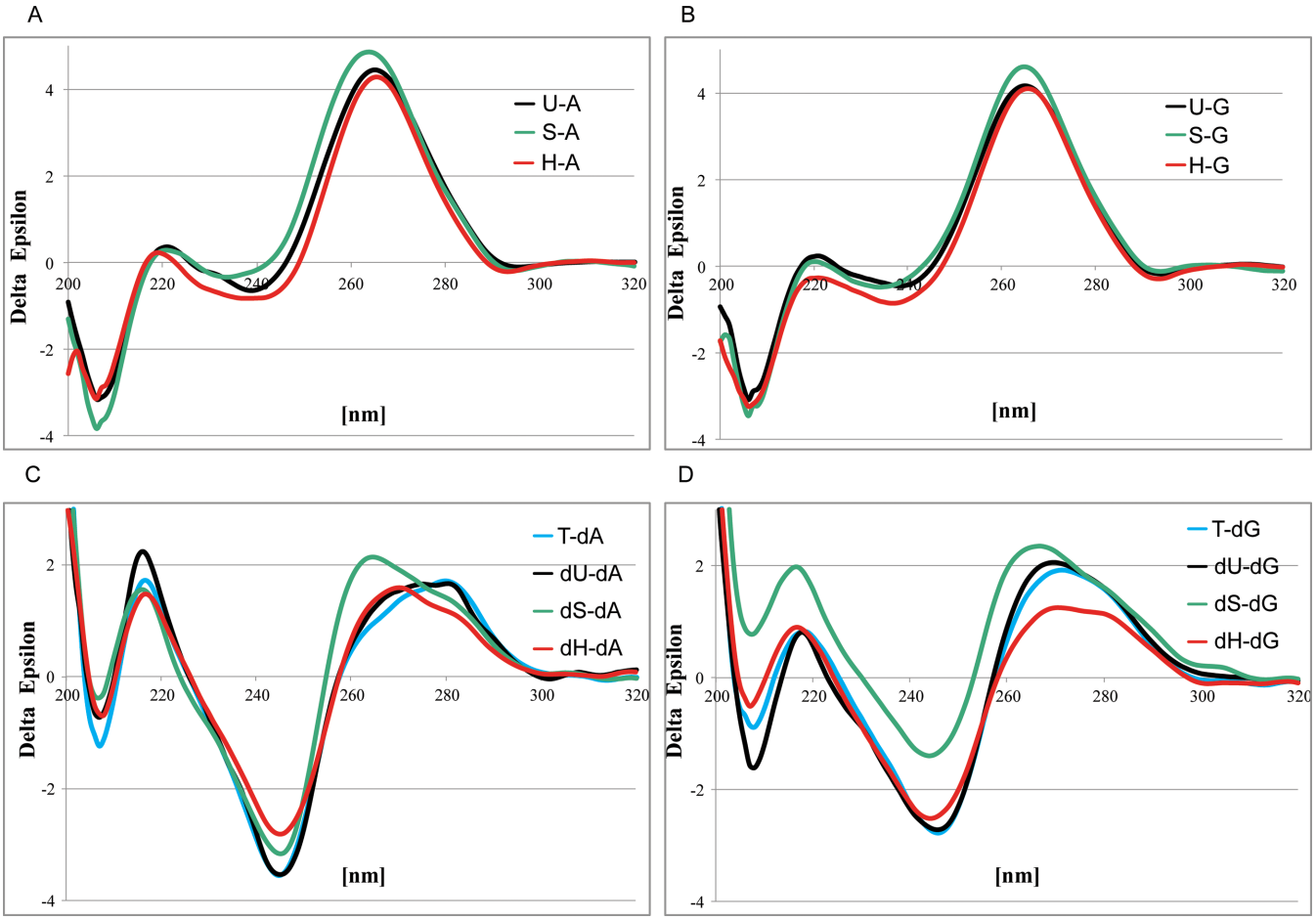

Figure 3. The CD spectra of RNA duplexes **1–3** (**A**) and **4–6** (**B**) as well as of DNA duplexes **7–10** (**C**) and **11–14** (**D**). The duplexes numbers and their abbreviated names are given in Table 1.

Interestingly, the most stable complex among the modeled base pairs was the H2U-G base pair shown in Figure 4F ($\Delta H = -10.0$ kcal/mol). The binding mode of this base pair differs from that of the typical U-G wobble base pair (WB, Figure 4D); therefore, we refer to this H2U-G base pair as a wobble* base pair (WB*) (Figure 4F). This base pair contains two hydrogen bonds formed between each of the HN(1) and HN(2) hydrogen atoms of G (the donors) and the O(4) and N(3) of H2U (the acceptors). The complex is not flat; the bases are twisted relative to each other by ∼33°, which is the result of the non-planarity of the exocyclic amine group in G involved in bonding. The bonding enthalpies (mean values) calculated for base pairs in an aqueous environment are 2–6 kcal/mol smaller than those in the gas phase (Supplementary Table S2). The observed binding destabilization in solution is due to the stronger solvation of individual bases, as previously observed (70). The qualitative order of relative bonding strengths is largely preserved, with the exception of the H2U-G wobble* base pair, which appears to be the most stabilized base pair upon solvation (i.e. the most strongly bound). Because this base pair is the only base pair discussed herein that has both hydrogen bonds pointed in the same direction, there is a larger net charge separation resulting in additional solvation stabilization. This stabilization partially compensates for the bond weakening effect (70).

The bonding energy of the S2U-G base pair (Figure 4E) is remarkably weaker compared with the U-G base pair because the sulfur atom forms a weaker hydrogen bond with the HN(1) group than with oxygen ($\Delta H = -7.5$ kcal/mol versus $\Delta H = -9.5$ kcal/mol) (67).

Models of the duplexes. Simple molecular mechanics calculations using an Amber96 force field were performed for the model RNA duplexes to estimate the impact of the H2U modified unit on the structure of the duplex and on the bonding energy between both strands in the helix. The optimized 9-bp RNAs contained each nucleoside in the C3′-*endo* sugar ring conformation with the exception of the H2U-modified unit, which was adjusted to adopt the C2′-*endo* sugar ring conformation. The calculations demonstrate that, in contrast to the unrestricted free base pair systems, the H2U-A base pair within the RNA chain does not form a structure resembling the wobble-like complex shown in Figure 4. In contrast, due to steric restrictions imposed by the chain and π–π stacking interactions (71), the complex adopted a Watson–Crick structure, as observed in the U-A base pair, but with only one hydrogen bond between the O(4) acceptor and the exocyclic HN(6) donor (Figure 5A).

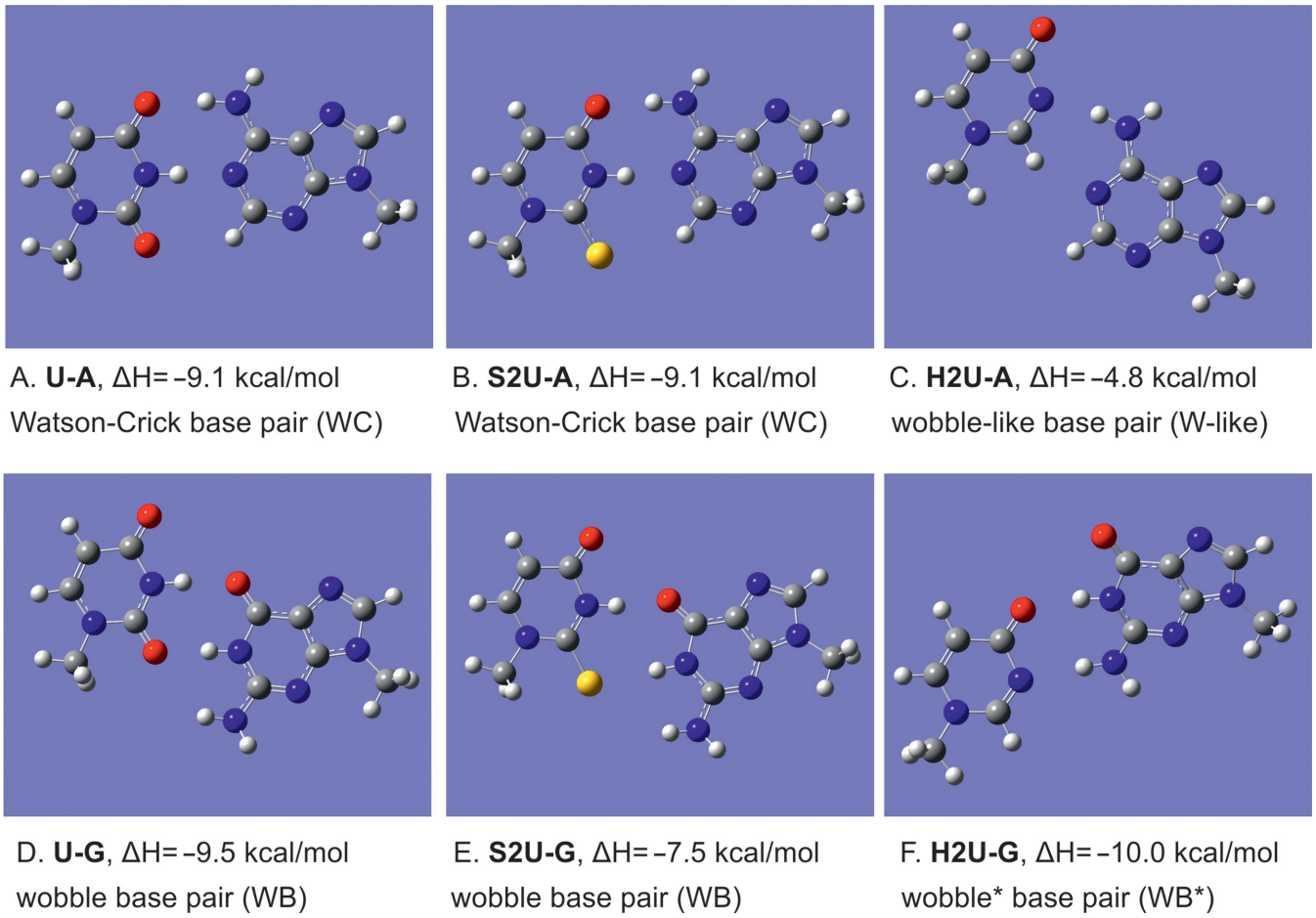

Figure 4. DFT modeling of the possible base pairs of U, S2U and H2U with A and G in water solution. In the used models the ribose residue of nucleoside is replaced with a methyl group. For the H2U-G base pair a stable two-hydrogen bonds base pair (F) is named as wobble* base pair, WB*.

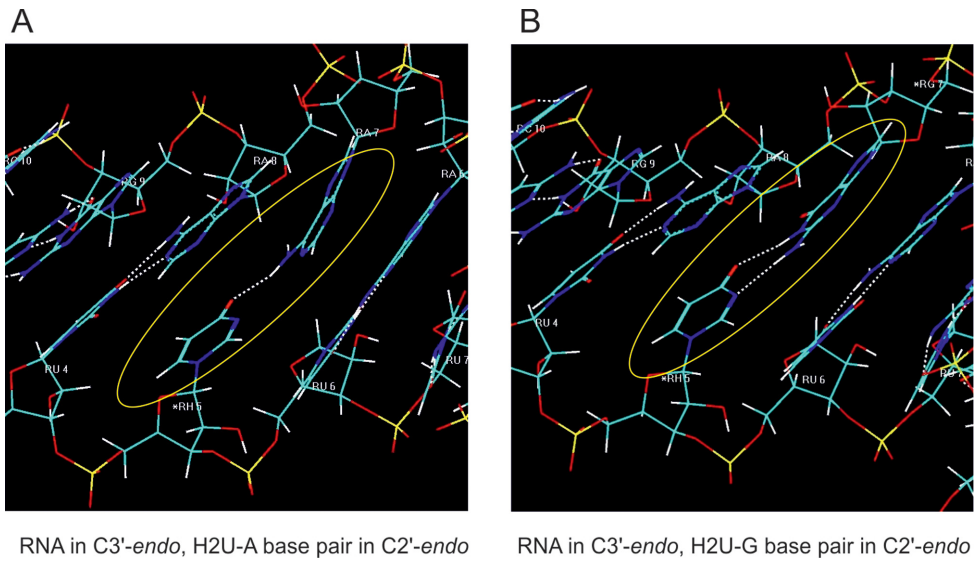

Figure 5. Fragments of the optimized 9-bp RNA duplexes 5′-GCU**H2U**UUAAC-3′/ 3′-CGA**A**/**G**AAUUG-5′ adopting the A-type helical structures, with modified base pairs marked: H2U-A (**A**) and H2U-G (**B**). The pictures show the RNA helixes with the base pairs adopting the C3′-*endo* sugar ring puckering, but with the H2U-A/G base pairing positioned in the C2′-*endo* sugar ring puckering.

In contrast, optimization of a 9-bp RNA duplex containing the H2U-G base pair (Figure 5B) indicates that the guanosine unit shifts to form wobble* bonding as has been suggested by DFT calculations. Because the crystallographic and nuclear magnetic resonance (NMR) analyses for H2U (46) suggest that the ribose attached to the 4-pyrimidinone base preferentially adopts the C2′-*endo* conformation, we modeled the C3′-*endo* RNA duplexes but with a C2′-*endo* conformation of the sugar moiety linked to the modified base. Interestingly, altering the ribose conformation of the H2U unit induces a similar conformational rearrangement from the C3′-*endo* to C2′-*endo* in the complementary A and G nucleosides upon optimization (Figure 5A and B). When modified base pairs are in the C2′-*endo* sugar ring conformation, the respective bases adopt buckle positioning (72). The models of isosequential DNA duplexes containing HdU-dA and HdU-dG base pairs are shown in the Supplementary Information (Supplementary Figure S3). The binding pattern and location of HdU-containing base pairs are analogous to those in the corresponding RNA models.

DISCUSSION

As observed for other sulfur-containing biomolecules, sulfur-containing nucleosides are prone to reaction with reactive oxygen species (73,74), which are produced during oxidative stress and may cause various lesions that alter biological processes in cells and in *in vitro* assays. Recently, we have demonstrated that in the presence of aqueous hydrogen peroxide, 2-thiouridine alone or within RNA chains undergoes efficient desulfuration according to an oxidative reduction mechanism (75). Interestingly, the process is pH dependent (44), and at lower pH (6.6), 2-thiouracil is predominantly transformed into 4-pyrimidinone, whereas at higher pH (7.6), uracil is the major product. Due to the specific characteristics of H2U (i.e. the donor/acceptor pattern and the C2′-*endo* sugar ring conformation that differ from those of S2U), its presence alters the binding affinity and structure of RNA and DNA double-stranded helices. This conclusion, which is suggested by our previous UV-melting analysis (45), is demonstrated in this study by DSC analysis and theoretical calculations.

The replacement of the 2-thiouracil residue with 4-pyrimidinone significantly reduces the thermodynamic stability of the corresponding **H-A** and **dH-dA** duplexes compared with the parent **S-A** and **dS-dA** duplexes. The respective ΔT_m values, $\Delta T_{m\mathbf{S\text{-}A/H\text{-}A}} = 7.2^\circ$C (Table 2) and $\Delta T_{m\mathbf{dS\text{-}dA/dH\text{-}dA}} = 13.2^\circ$C (Table 3), indicate that the stability of the DNA duplex is altered to a greater extent by the removal of the thiocarbonyl function than that of the corresponding RNA duplex. This result leads to the question of how the 4-pyrimidinone-adenine base pair is arranged within the RNA and DNA duplexes. Upon DFT optimization, this base pair formed a separated Watson–Crick base pair that does not reach an energy minimum in either aqueous solution or the gas phase. Rather, the formation of a wobble-like base pair ($\Delta H = -4.8$ kcal/mol, Figure 4C) that contains a typical hydrogen bond between the nitrogen N(3) atom in 4-pyrimidinone and the HN(6) function in adenine appears to be possible, in addition to a weak stabilizing interaction between the C(2)H of the 4-pyrimidinone moiety and the endocyclic N(1) nitrogen acceptor of adenine. However, MM Amber calculations of a model 9-bp A-type RNA duplex (Figure 5A) suggest that the unstable H2U-A base pair accommodates in the double helix in the same manner as an isosteric S2U-A base pair. Adjustment of the C2′-*endo* sugar ring conformation of the H2U residue induces the conformational rearrangement C3′-*endo*→C2′-*endo* in the complementary adenosine. In addition to possible π–π stacking interactions (71), the H2U-A base pair within the RNA chain is stabilized by only one WC isosteric hydrogen bond (Figure 6A) (76). The bases are twisted to reduce the repulsive interaction between the lone electron pairs in the nitrogen atoms N(3) of 4-pyrimidinone and N(1) of adenine (47,77). Nevertheless, these computational results are only weakly reflected in the CD spectra of H2U-A and H2dU-dA, which are nearly identical to those determined for their sulfur-containing precursors (Figure 3A and C).

When S2U in the **S-G** duplex is replaced with a 4-pyrimidinone riboside, the melting temperature of the resulting **H-G** is close to that of **S-G**. The observed decrease in T_m is much smaller than that observed for **S-A**→**H-A** duplexes, and the T_m for **H-G** is slightly higher than the T_m value for **H-A**. Interestingly, the analogous **dH-dG** DNA duplex is much more stable than the parent **dS-dG** duplex. These results are in contrast to those obtained for the **dH-dA** duplex, which exhibited much weaker stability than that of the sulfur-containing congener. Initially, this result appears remarkable because the wobble topology (analogous to that in **S-G**, Figure 6B) disallows any hydrogen bonding between 4-pyrimidinone and guanine. However, as we have observed from DFT modeling, isolated 4-pyrimidinone-guanine base pairs are the most stable when arranged in the WB* mode (Figure 4F). This base pair exploits two hydrogen bonds of identical polarity that are formed between both NH donors of G (N(1) and N(2)) and the O(4) and N(3) acceptors of H2U. However, to form this H2U-G base pair, the RNA helix requires a conformational rearrangement, i.e. movement of the wobble H2U base along the y-axis to the WB* location. This shift provides two new hydrogen bonds, which are energetically equivalent to the original wobble hydrogen bonds between U and G ($\Delta H = -9.5$ kcal/mol for U-G WB versus $\Delta H = -10.0$ kcal/mol for H2U-G WB*). Our Molecular Mechanics (MM) calculations provide evidence that the WB* arrangement does not distort the RNA helix (Figure 6); thus, **H-G** is only slightly less stable than the parent **U-G** ($\Delta T_m = 2.5^\circ$C and $\Delta\Delta G_{25} = 4.1$ kcal/mol). Indeed, a superposition of the MM-optimized structures of U-G- and H2U-G-containing duplexes (Supplementary Figure S2) reveals the translation of the 4-pyrimidinone riboside along the y-axis of the helix and the rotation of the H2U and G bases to adopt the arrangement suitable for efficient base pairing. The structures of the HdU-dA and HdU-dG base pairs in isosequential DNA duplexes are analogous to those in the U-G- and H2U-G-containing duplexes (Supplementary Figure S3).

There is an additional and perhaps more important aspect of the discussed desulfuration. We searched for examples in the literature of preferential G (versus A) recognition by 2-oxo/thioalkylated uridine/thymidine units. In-

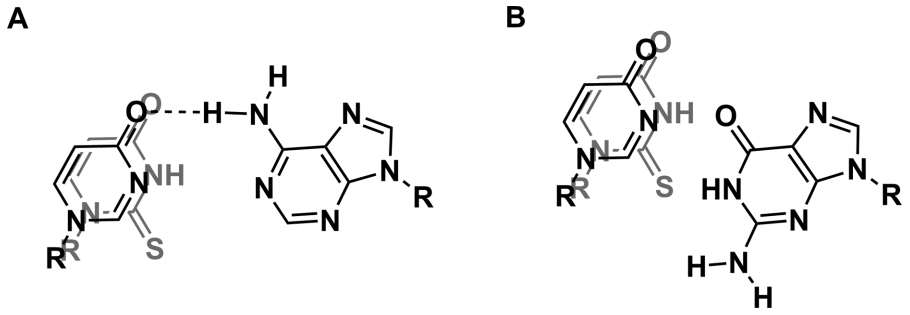

Figure 6. Structures of the H2U-A and H2U-G base pairs located in the topologic site of the parent Watson–Crick S2U-A and classical wobble S2U-G base pairs (with structure of the parent S2U shown in gray).

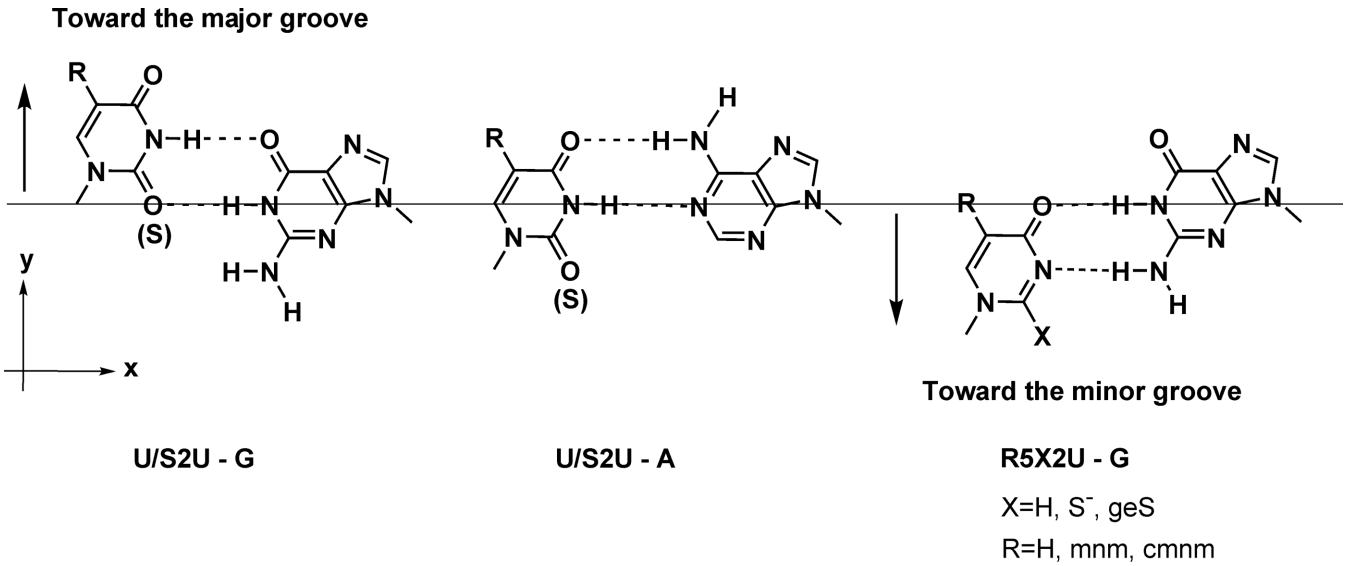

Figure 7. Proposed topology of the base pairs according to the classical mode of Watson–Crick, a wobble mode (a pyrimidine unit directed toward the major groove) and WB* (a pyrimidine unit directed toward the minor groove), according to Takai (86). The U/S2U-A, U/S2U-G and X2U-G base pairs are positioned within the RNA helix (R = H or (c)mnm and X = S^-, geS or H).

terestingly, in all identified cases, the modified pyrimidines possess a 4-pyrimidinone-type scaffold (containing a system of double bonds and hydrogen bond acceptors as in H2U), which, consistent with our hypothesis, may interact with guanine according to the WB* pairing mode. One example concerns 11-bp DNA duplexes containing O(2)-methyl thymidine, which preferentially interact with guanine rather than adenine (78). Furthermore, O(2)-alkylated thymidines are considered mutagenic lesions in DNA (79) because O(2)-alkylated thymidines in DNA templates are not accepted by DNA polymerase (80,81), which inhibits DNA replication and leads to non-coding lesions. Notably, the incorporation of thymidine lacking the 2-carbonyl function into DNA sequences destabilizes base pairing with dA (47).

A second example comes from studies on codon–anticodon interactions, which are important for the translation process in which hypermodified 2-thiouridines (located in the wobble position of anticodon of tRNAs) provide precise reading of the third letter of the codon either by Watson–Crick base pairing with A or by wobble pairing with G. Recently, new hypermodified nucleosides containing the 4-pyrimidinone motif generated by alkylation of the 2-thiocarbonyl function have been discovered. These *S*-geranyl-2-thiouridines, which are substituted with 5-methylaminomethyl (mnm) or 5-carboxymethylaminomethyl (cmnm) groups (Figure 7; in the structure on the right, X = geS, R = mnm or cmnm), are located in the wobble position of tRNAs specific for Lys, Glu and Gln and were identified in several bacterial strains exposed to cellular stress (82). A comparison of the translation efficiency of the glutamate codons 5′-GAA and 5′-GAG at varying degrees of geranylation revealed that the GAA/GAG translation efficiency ratio was altered from 13:1 to 6:1, indicating the preferred reading of G-ending codons (82).

This change in reading preference from A- to G-ending codons was also observed for a tRNA with a wobble mnm5S2U nucleoside (83,84). As hypothesized by Takai and Yokoyama (85), the 5-methylaminomethyl substituent of the 2-thiouracil moiety may be protonated at the amino function at physiological pH, whereas the sulfur atom carries a negative charge. An altered electronic structure of the zwitterionic mnm5S2U results in the formation of a

4-pyrimidinone-type nucleoside (R5X2U) in which the N3 atom becomes a hydrogen bond acceptor (Figure 7, R = (c)mnm, X = S^-). Takai further postulated that the aforementioned wobble pyrimidine nucleosides may decode the third letter of codons in the new wobble geometry (denoted wobble*, WB*), in which the pyrimidine nucleoside is shifted toward the minor groove (Figure 7) (86). This interaction is suggested to be similarly effective as the Watson–Crick base pairing and classical wobble base pairing in which pyrimidine nucleosides are shifted toward the major groove compared with the pyrimidine position in the Watson–Crick arrangement. However, we demonstrate that this new wobble arrangement is only possible if the pyrimidine nucleoside adopts the H2U-type structure. Thus, tRNAs modified with an H2U-type wobble nucleoside (obtained either by its protonation and charge localization at the sulfur moiety or by sulfur alkylation) preferentially recognize G as the third letter of the codon, not A. We suggest that this 3′-G-ending codon reading may occur through the WB* interactions favored in the H2U-G base pair via translation of the H2U-type wobble nucleoside along the y-axis of the WB* geometry (Figure 7, right base pair), unless accommodation of this base pair is possible within the ribosomal context (87,88).

Although it is not strictly connected with our model, note that 3′-G-ending codons are also recognized by tRNAs containing a 5-methoxycarbonylmethyl-2-thiouridine (mcm5S2U) wobble nucleoside (89). However, based on crystallographic and NMR spectral studies, this characteristic is attributed to the specific binding pattern of guanine with the C(4)-keto-enol tautomer of the mcm5S2U unit (90).

Three U-G base pair spatial arrangements that are similar to our H2U-G wobble* model have emerged from crystal structures of *T. thermophilus* 30S and archaeal *Haloarcula marismortui* ribosomal RNA (91). However, despite the striking similarity in the spatial orientation, both models differ in the number of identified hydrogen bonds (only one hydrogen bond between the uracil O(4) and H-N(1) of guanine is present instead of two in the H2U-G base pair). Nevertheless, the translation of the uridine base along the y-axis is observed in the crystal structures.

In conclusion, our studies demonstrate that the preferred binding of S2U with A is lost upon its desulfuration to a 4-pyrimidinone nucleoside. Moreover, the preferred binding of H2U with a guanosine partner is observed. Thus, biological processes and *in vitro* assays in which oxidative desulfuration of the 2-thiouracil-containing component may occur may be altered with unpredictable consequences. The proposed binding pattern of the 4-pyrimidinone–guanine base pair contains two hydrogen bonds between the O(4) and N(3) acceptors of the 4-pyrimidinone and the two NH donors of guanine and can be adopted only by proper spatial arrangement of both bases. This arrangement can be achieved by translation of the H2U nucleoside into the minor groove compared with the topology of the classical U-G wobble base pair (arranged in the major grove compared with the WC base pair). As a biological consequence, the tRNA wobble nucleosides in the anticodon, which under physiological conditions are able to adopt the 4-pyrimidinone-type double bond system, may preferentially read 3′-G-ending codons rather than A-ending codons. To the best of our knowledge, this is the first thermodynamic and theoretical study suggesting the existence of WB* in an experimental system.

SUPPLEMENTARY DATA

Supplementary Data are available at NAR Online.

ACKNOWLEDGEMENT

The authors thank Dr Piotr Guga for constructive suggestions and help in the article editing.

FUNDING

National Science Centre in Poland [UMO-2011/03/B/ST5/02669 to B.N. and E.S. for 2012–2015]; Centre of Molecular and Macromolecular Studies of the Polish Academy of Sciences and Technical University of Lodz, Poland; PL-Grid Infrastructure. Funding for open access charge: National Science Centre in Poland [UMO-2011/03/B/ST5/02669].
Conflict of interest statement. None declared.

REFERENCES

1. Machnicka,M.A., Milanowska,K., Osman Oglou,O., Purta,E., Kurkowska,M., Olchowik,A., Januszewski,W., Kalinowski,S., Dunin-Horkawicz,S., Rother,K.M. *et al.* (2013) MODOMICS: a database of RNA modification pathways–2013 update. *Nucleic Acids Res.*, **41**, D262–D267.
2. Cantara,W.A., Crain,P.F., Rozenski,J., McCloskey,J.A., Harris,K.A., Zhang,X., Vendeix,F.A., Fabris,D. and Agris,P. F. (2011) The RNA modification database, RNAMDB: 2011 update. *Nucleic Acids Res.*, **39**, D195–D201.
3. Agris,P.F., Vendeix,F.A. and Graham,W.D. (2007) tRNA's wobble decoding of the genome: 40 years of modification. *J. Mol. Biol.*, **366**, 1–13.
4. Agris,P.F. (2008) Bringing order to translation: the contributions of transfer RNA anticodon-domain modifications. *EMBO Rep.*, **9**, 629–635.
5. Yokoyama,S. and Nishimura,S. (1995) Modified nucleosides and codon recognition. In: Söll,D and RajBhandary,U (eds). *tRNA: Structure, Biosynthesis, and Function*. American Society for Microbiology, Washington, DC, pp. 207–223.
6. Curran,J.F. (1998) Modified nucleosides in translation. In: Grosjean,H and Benne,R (eds). *Modification and Editing of RNA*. ASM Press, Washington, DC, pp. 493–516.
7. Watanabe,K. (2007) Role of modified nucleosides in the translation function of tRNAs from extreme thermophilic bacteria and animal mitochondria. *Bull. Chem. Soc. Japan*, **80**, 1253–1267.
8. Shigi,N. (2014) Biosynthesis and functions of sulphur modifications in tRNA. *Front. Genet.*, **5**, 1–11.
9. Jackman,J.E. and Alfonzo,J.D. (2013) Transfer RNA modifications: nature's combinatorial chemistry playground. *Wiley Interdiscip. Rev. RNA*, **4**, 35–48.
10. Madore,E., Florentz,C., Giegé,R., Sekine,S., Yokoyama,S. and Lapointe,J. (1999) Effect of modified nucleotides on Escherichia coli tRNAGlu structure and on its aminoacylation by glutamyl-tRNA synthetase. Predominant and distinct roles of the mnm5 and s2 modifications of U34. *Eur. J. Biochem.*, **266**, 1128–1135.
11. Sylvers,L.A., Rogers,K.C., Shimizu,M., Ohtsuka,E. and Söll,D. (1993) A 2-thiouridine derivative in tRNAGlu is a positive determinant for aminoacylation by Escherichia coli glutamyl-tRNA synthetase. *Biochemistry*, **32**, 3836–3841.
12. Karikó,K., Buckstein,M., Ni,H. and Weissman,D. (2005) Suppression of RNA recognition by Toll-like receptors: the impact of nucleoside modification and the evolutionary origin of RNA. *Immunity*, **23**, 165–175.

13. Nallagatla,S.R. and Bevilacqua,P.C. (2008) Nucleoside modifications modulate activation of the protein kinase PKR in an RNA structure-specific manner. *RNA*, **14**, 1201–1213.
14. Nallagatla,S.R., Jones,C.N., Ghosh,S.K., Sharma,S.D., Cameron,C.E., Spremulli,L.L. and Bevilacqua,P.C. (2013) Native tertiary structure and nucleoside modifications suppress tRNA's intrinsic ability to activate the innate immune sensor PKR. *PLoS One*, **8**, e57905.
15. Isel,C., Marquet,R., Keith,G., Ehresmann,C. and Ehresmann,B. (1993) Modified nucleotides of tRNA(3Lys) modulate primer/template loop-loop interaction in the initiation complex of HIV-1 reverse transcription. *J. Biol. Chem.*, **268**, 25269–25272.
16. Watanabe,K., Oshima,T., Saneyoshi,M. and Nishimura,S. (1974) Replacement of ribothymidine by 5-methyl-2-thiouridine in sequence GT psi C in tRNA of an extreme thermophile. *FEBS Lett.*, **43**, 59–63.
17. Sprinzl,M., Horn,C., Brown,M., Ioudovitch,A. and Steinberg,S. (1998) Compilation of tRNA sequences and sequences of tRNA genes. *Nucleic Acids Res.*, **26**, 148–153.
18. Kowalak,J.A., Dalluge,J.J., McCloskey,J.A. and Stetter,K.O. (1994) The role of posttranscriptional modification in stabilization of transfer RNA from hyperthermophiles. *Biochemistry*, **33**, 7869–7876.
19. Sierzputowska-Gracz,H., Sochacka,E., Malkiewicz,A., Kuo,K., Gehrke,C.W. and Agris,P.F. (1987) Chemistry and structure of modified uridines in the anticodon, wobble position of transfer RNA are determined by thiolation. *J. Am. Chem. Soc.*, **109**, 7171–7177.
20. Agris,P.F., Sierzputowska-Gracz,H., Smith,W., Malkiewicz,A., Sochacka,E. and Nawrot,B. (1992) Thiolation of uridine carbon-2 restricts the motional dynamics of the transfer RNA wobble position nucleoside. *J. Am. Chem. Soc.*, **114**, 2652–2656.
21. Yamamoto,Y., Yokoyama,S., Miyazawa,T., Watanabe,K. and Higuchi,S. (1983) NMR analyses on the molecular mechanism of the conformational rigidity of 2-thioribothymidine, a modified nucleoside in extreme thermophile tRNAs. *FEBS Lett.*, **157**, 95–99.
22. Sundaram,M., Durant,P.C. and Davis,D.R. (2000) Hypermodified nucleosides in the anticodon of $tRNA^{Lys}$ stabilize a canonical U-turn structure. *Biochemistry*, **39**, 12575–12584.
23. Testa,S.M., Disney,M.D., Turner,D.H. and Kierzek,R. (1999) Thermodynamics of RNA-RNA duplexes with 2- or 4-thiouridines: implications for antisense design and targeting a group I intron. *Biochemistry*, **38**, 16655–16662.
24. Kumar,R.K. and Davis,D.R. (1997) Synthesis and studies on the effect of 2-thiouridine and 4-thiouridine on sugar conformation and RNA duplex stability. *Nucleic Acids Res.*, **25**, 1272–1280.
25. Shohda,K., Okamoto,I., Wada,T., Seio,K. and Sekine,M. (2000) Synthesis and properties of 2′-O-methyl-2-thiouridine and oligoribonucleotides containing 2′-O-methyl-2-thiouridine. *Bioorg. Med. Chem. Lett.*, **10**, 1795–1798.
26. Okamoto,I., Seio,K. and Sekine,M. (2006) Incorporation of 2′-O-methyl-2-thiouridine into oligoribonucleotides induced stable A-form structure. *Chem. Lett.*, **35**, 136–137.
27. Sipa,K., Sochacka,E., Kazmierczak-Baranska,J., Maszewska,M., Janicka,M., Nowak,G. and Nawrot,B. (2007) Effect of base modifications on structure, thermodynamic stability, and gene silencing activity of short interfering RNA. *RNA*, **13**, 1301–1316.
28. Sierant,M., Paduszynska,A., Kazmierczak-Baranska,J., Nacmias,B., Sorbi,S., Bagnoli,S., Sochacka,E. and Nawrot,B. (2011) Specific silencing of L392V PSEN1 mutant allele by RNA interference. *Int. J. Alzheimers Dis.*, **2011**, 809218.
29. Prakash,T.P., Naik,N., Sioufi,N., Bhat,B. and Swayze,E.E. (2009) Activity of siRNAs with 2-thio-2′-O-methyluridine modification in mammalian cells. *Nucleosides Nucleotides Nucleic Acids*, **28**, 902–910.
30. Polak,M., Manoharan,M., Inamati,G.B. and Plavec,J. (2003) Tuning of conformational preorganization in model 2′, 5′- and 3′, 5′-linked oligonucleotides by 3′- and 2′-O-methoxyethyl modification. *Nucleic Acids Res.*, **31**, 2066–2076.
31. Okamoto,I., Seio,K. and Sekine,M. (2008) Study of the base discrimination ability of DNA and 2′-O-methylated RNA oligomers containing 2-Thiouracil BNases towards complementary RNA or DNA starands and their application to single-base mismatch detection. *Bioorg. Med. Chem.*, **16**, 6034–6041.
32. Kierzek,E., Kierzek,R., Turner,D.H. and Catrina,I.E. (2006) Facilitating RNA structure prediction with microarrays. *Biochemistry*, **45**, 581–593.
33. Diop-Frimpong,B., Prakash,T.P., Rajeev,K.G., Manoharan,M. and Egli,M. (2005) Stabilizing contributions of sulphur-modified nucleotides: crystal structure of a DNA duplex with 2′-O-[2-(methoxy)ethyl]-2-thiothymidines. *Nucleic Acids Res.*, **33**, 5297–5307.
34. Ivanov,A.A., Ko,H., Cosyn,L., Maddileti,S., Besada,P., Fricks,I., Costanzi,S., Harden,T.K., Calenbergh,S.V. and Jacobson,K.A. (2007) Molecular modeling of the human P2Y2 receptor and design of a selective agonist, 2′-amino-2′-deoxy-2-thiouridine 5′-triphosphate. *J. Med. Chem.*, **50**, 1166–1176.
35. Ko,H., Carter,L., Cosyn,L., Petrelli,R., de Castro,S., Besada,P., Zhou,Y., Cappellacci,L., Franchetti,P., Grifantini,M. *et al.* (2008) Synthesis and potency of novel uracil nucleotides and derivatives as P2Y2 and P2Y6 receptor agonists. *Bioorg. Med. Chem.*, **16**, 6319–6332.
36. Das,A., Ko,H., Burianek,L.E., Barrett,M.O., Harden,T.K. and Jacobson,K.A. (2010) Human P2Y(14) receptor agonists: truncation of the hexose moiety of uridine-5′-diphosphoglucose and its replacement with alkyl and aryl groups. *J. Med. Chem.*, **53**, 471–480.
37. Bretner,M., Kulikowski,T., Dzik,J.M., Balińska,M., Rode,W. and Shugar,D. (1993) 2-Thio derivatives of dUrd and 5-fluoro-dUrd and their 5′-monophosphates: synthesis, interaction with tumor thymidylate synthase, and in vitro antitumor activity. *J. Med. Chem.*, **36**, 3611–3617.
38. Kuimelis,R.G. and Nambiar,K.P. (1994) Synthesis of oligodeoxynucleotides containing 2-thiopyrimidine residues-a new protection scheme. *Nucleic Acids Res.*, **22**, 1429–1436.
39. Connolly,B.A. and Newman,P.C. (1989) Synthesis and properties of oligonucleotides containing 4-thiothymidine, 5-methyl-2-pyrimidinone-1-beta-D(2′-deoxyriboside) and 2-thiothymidine. *Nucleic Acids Res.*, **17**, 4957–4974.
40. Newman,P.C., Nwosu,V.U., Williams,D.M., Cosstick,R., Seela,F. and Connolly,B.A. (1990) Incorporation of a complete set of deoxyadenosine and thymidine analogues suitable for the study of protein nucleic acid interactions into oligodeoxynucleotides. Application to the EcoRV restriction endonuclease and modification methylase. *Biochemistry*, **29**, 9891–9901.
41. Sintim,H.O. and Kool,E.T. (2006) Enhanced base pairing and replication efficiency of thiothymidines, expanded-size variants of thymidine. *J. Am. Chem. Soc.*, **128**, 396–397.
42. Sismour,A.M. and Benner,S.A. (2005) The use of thymidine analogs to improve the replication of an extra DNA base pair: a synthetic biological system. *Nucleic Acids Res.*, **33**, 5640–5646.
43. Hoshika,S., Chen,F., Leal,N.A. and Benner,S.A. (2008) Self-Avoiding Molecular Recognition Systems (SAMRS). *Nucleic Acids Symp. Ser. (Oxf)*, **52**, 129–130.
44. Sochacka,E., Bartos,P., Kraszewska,K. and Nawrot,B. (2013) Desulphuration of 2-thiouridine with hydrogen peroxide in the physiological pH range 6.6–7.6 is pH-dependent and results in two distinct products. *Bioorg. Med. Chem. Lett.*, **23**, 5803–5805.
45. Sochacka,E., Kraszewska,K., Sochacki,M., Sobczak,M., Janicka,M. and Nawrot,B. (2011) The 2-thiouridine unit in the RNA strand is desulphured predominantly to 4-pyrimidinone nucleoside under in vitro oxidative stress conditions. *Chem. Commun.*, **47**, 4914–4916.
46. Kraszewska,K., Kaczyńska,I., Jankowski,S., Karolak-Wojciechowska,J. and Sochacka,E. (2011) Desulphurization of 2-thiouracil nucleosides: conformational studies of 4-pyrimidinone nucleosides. *Bioorg. Med. Chem.*, **19**, 2443–2449.
47. Guo,M.J., Hildbrand,S., Leumann,C.J., McLaughlin,L.W. and Waring,M.J. (1998) Inhibition of DNA polymerase reactions by pyrimidine nucleotide analogues lacking the 2-keto group. *Nucleic Acids Res.*, **26**, 1863–1869.
48. Sochacka,Nawrot.B. and Düchler,M. (2011) tRNA structural and functional changes induced by oxidative stress. *Cell Mol. Life Sci.*, **68**, 4023–4032.
49. Thompson,D.M., Lu,C., Green,P.J. and Parker,R. (2008) tRNA cleavage is a conserved response to oxidative stress in eukaryotes. *RNA.*, **14**, 2095–2103.
50. Nawrot,B. and Sochacka,E. (2009) Preparation of short interfering RNA containing the modified nucleosides 2-thiouridine, pseudouridine, or dihydrouridine. *Curr. Protoc. Nucleic Acid Chem.*, Chapter 16, Unit 16.2.
51. Sochacka,E. and Fratczak,I. (2004) Efficient desulphurization of 2-thiopyrimidine nucleosides to corresponding 4-pyrimidinone

analogues using trans-2-phenylsulfonyl-3-phenyloxaziridine. *Tetrahedron Lett.*, **45**, 6729–6731.
52. Zon,G. and Stec,W.J. (1991) Phosphorothioate oligonucleotides. In: Eckstein,F (ed). *Oligonucleotides and Analogues: A Practical Approach*. IRL Press, London, pp. 87–108.
53. Borer,P.N. (1975) Optical properties of nucleic acids, absorption and circular dichroism spectra. In: Fasman,GD (ed). *Handbook of Biochemistry and Molecular Biology: Nucleic Acids*. 3rd edn. CRC Press, Cleveland, OH, Vol. **1**, pp. 589–590.
54. Richards,E.G. (1975). Use of tables in calculation of absorption, optical rotatory dispersion and circular dichroism of polyribonucleotides. In: Fasman,GD (ed). *Handbook of Biochemistry and Molecular Biology: Nucleic Acids*. 3rd edn. CRC Press, Cleveland, OH, Vol. **1**, pp. 596–603.
55. Jelesarov,I., Crane-Robinson,C. and Privalov,P. (1999) The energetics of HMG box interactions with DNA: thermodynamic description of the target DNA duplexes. *J. Mol. Biol.*, **294**, 981–995.
56. Marky,L.A. and Breslauer,K.J. (1987) Calculating thermodynamic data for transitions of any molecularity from equilibrium melting curves. *Bioploymers*, **26**, 1601–1620.
57. Frisch,M.J., Trucks,G.W., Schlegel,H.B., Scuseria,G.E., Robb,M.A., Cheeseman,J.R., Scalmani,G., Barone,V., Mennucci,B., Petersson,G.A. *et al.* (2009) *Gaussian 09, Revision D.01*. Gaussian, Inc., Wallingford CT.
58. Chai,J.D. and Head-Gordon,M. (2008) Long-range corrected hybrid density functionals with damped atom-atom dispersion corrections. *Phys. Chem. Chem. Phys.*, **10**, 6615–6620.
59. Kollman,P.A. (1996) Advances and continuing challenges in achieving realistic and predictive simulations of the properties of organic and biological molecules. *Acc. Chem. Res.*, **29**, 461–469.
60. Vallone,P.M., Paner,T.M., Hilario,J., Lane,M.J., Faldasz,B.D. and Benight,A.S. (1999) Melting studies of short DNA hairpins: influence of loop sequence and adjoining base pair identity on hairpin thermodynamic stability. *Biopolymers*, **50**, 425–442.
61. Kuijpers,W.H.A., Kuyl-Yeheskiely,E., van Boom,J.H. and van Boeckel,C.A.A. (1993) The application of the AMB protective group in the solid phase synthesis of methylphosphonate DNA analogues. *Nucleic Acids Res.*, **21**, 3493–3500.
62. Wells,B.D. and Yang,J.T. (1974) A computer probe of the circular dichroic bands of nucleic acids in the ultraviolet region. I. Transfer ribonucleic acid. *Biochemistry*, **13**, 1311–1316.
63. Johnson,W.C. (1996) *Determination of the Conformation of Nucleic Acids by Electronic CD*. Plenum Press, NY.
64. Šponer,J., Jurečka,P. and Hobza,P. (2004) Accurate interaction energies of hydrogen-bonded nucleic acid base pairs. *J. Am. Chem. Soc.*, **126**, 10142–10151.
65. Šponer,J., Šponer,J.E., Mládek,A., Banáš,P., Jurečka,P. and Otyepka,M. (2013) How to understand quantum chemical computations on DNA and RNA systems? A practical guide for non-specialists. *Methods*, **64**, 3–11.
66. Kawahara,S., Wada,T., Kawauchi,S., Uchimaru,T. and Sekine,M. (1999) Ab initio and density functional studies of substituent effects of an A-U base pair on the stability of hydrogen bonding. *J. Phys. Chem. A*, **103**, 8516–8523.
67. Masaki,Y., Miyasaka,R., Hirai,K., Kanamori,T., Tsunoda,H., Ohkubo,A., Seio,K. and Sekine,M. (2014) Properties of 5- and/or 2-modified 2′-Ocyanoethyl uridine residue: 2′-O-cyanoethyl-5-propynyl-2-thiouridine as an efficient duplex stabilizing component. *Org. Biomol. Chem.* **12**, 1157–1162.
68. Scheiner,S. (2005) The CH–O hydrogen bond. A historical account. In: Dykstra,CE, Frenking,G, Kim,KS and Scuseria,GE (eds). *Theory and Applications of Computational Chemistry: The First 40 Years*. Elsevier, Amsterdam, pp. 831–857.
69. Gu,Y., Kar,T. and Scheiner,S. (2000) Comparison of the CH…N and CH…O interactions involving substituted alkanes. *J. Mol. Struct.*, **552**, 17–31.
70. Poater,J., Swart,M., Guerra,C.F. and Bickelhaupt,F.M. (2012) Solvent effects on hydrogen bonds in Watson–Crick, mismatched, and modified DNA base pairs. *Comp. Theor. Chem.*, **998**, 57–63.
71. Kool,E.T. (2001) Hydrogen bonding, base stacking, and steric effects in DNA replication. *Annu. Rev. Biophys. Biomol. Struct.*, **30**, 1–22.
72. Olson,W.K., Bansal,M., Burley,S.K., Dickerson,R.E., Gerstein,M., Harvey,S.C., Heinemann,U., Lu,X.J., Neidle,S., Shakked,Z. *et al.* (2001) A standard reference frame for the description of nucleic acid base-pair geometry. *J. Mol. Biol.*, **313**, 229–237.
73. Battin,E.E. and Brumaghim,J.L. (2009) Antioxidant activity of sulphur and selenium: a review of reactive oxygen species scavenging, glutathione peroxidase, and metal-binding antioxidant mechanisms. *Cell Biochem. Biophys.*, **55**, 1–23.
74. Xie,X., Liang,J., Pu,T., Xu,F., Yao,F., Yang,Y., Zhao,Y.L., You,D., Zhou,X., Deng,Z. *et al.* (2012) Phosphorothioate DNA as an antioxidant in bacteria. *Nucleic Acids Res.*, **40**, 9115–9124.
75. Schantl,J.G. and Lagoja,I.M. (1998) 1-arylamino-1H-imidazoles by 'oxidative reduction' - Conversion of 1-arylamino-2, 3-dihydro-1H-Imidazole-2-thiones. *Heterocycles*, **48**, 929–938.
76. Westhof,E. (2014) Isostericity and tautomerism of base pairs in nucleic acids. *FEBS Lett.*, **588**, 2464–2469.
77. Ono,A., Torigoe,H., Tanaka,Y. and Okamoto,I. (2011) Binding of metal ions by pyrimidine base pairs in DNA duplexes. *Chem. Soc. Rev.*, **40**, 5855–5866.
78. Xu,Y.Z. and Swann,P.F. (1994) Oligodeoxynucleotides containing O2-alkylthymine: synthesis and characterization. *Tetrahedron Lett.*, **35**, 303–306.
79. Singer,B. (1976) All oxygens in nucleic acids react with carcinogenic ethylating agents. *Nature*, **264**, 333–339.
80. Grevatt,P.C., Solomon,J.J. and Bhanot,O.S. (1992) In vitro mispairing specificity of O2-ethylthymidine. *Biochemistry*, **31**, 4181–4188.
81. Bhanot,O.S., Grevatt,P.C., Donahue,J.M., Gabrielides,C.N. and Solomon,J.J. (1992) In vitro DNA replication implicates O2-ethyldeoxythymidine in transversion mutagenesis by ethylating agents. *Nucleic Acids Res.*, **20**, 587–594.
82. Dumelin,C.E., Chen,Y., Leconte,A.M., Chen,Y.G. and Liu,D.R. (2012) Discovery and biological characterization of geranylated RNA in bacteria. *Nat. Chem. Biol.*, **8**, 913–919.
83. Krüger,M.K., Pedersen,S., Hagervall,T.G. and Sørensen,M.A. (1998) The modification of the wobble base of tRNAGlu modulates the translation rate of glutamic acid codons in vivo. *J. Mol. Biol.*, **284**, 621–631.
84. Yarian,C., Marszalek,M., Sochacka,E., Malkiewicz,A., Guenther,R., Miskiewicz,A. and Agris,P.F. (2000) Modified nucleoside dependent Watson-Crick and wobble codon binding by tRNALysUUU species. *Biochemistry*, **39**, 13390–13395.
85. Takai,K. and Yokoyama,S. (2003) Roles of 5-substituents of tRNA wobble uridines in the recognition of purine-ending codons. *Nucleic Acids Res.*, **31**, 6383–6391.
86. Takai,K. (2006) Classification of the possible pairs between the first anticodon and the third codon positions based on a simple model assuming two geometries with which the pairing effectively potentiates the decoding complex. *J. Theor. Biol.*, **242**, 564–580.
87. Demeshkina,N., Jenner,L., Westhof,E., Yusupov,M. and Yusupova,G. (2012) A new understanding of the decoding principle on the ribosome. *Nature*, **484**, 256–259.
88. Schmeing,T.M., Voorhees,R.M., Kelley,A.C., Gao,Y.G., Murphy,F.V. 4th, Weir,J.R. and Ramakrishnan,V. (2009) The crystal structure of the ribosome bound to EF-Tu and aminoacyl-tRNA. *Science*, **326**, 688–694.
89. Johansson,M.J., Esberg,A., Huang,B., Bjork,G.R. and Bystrom,A.S. (2008) Eukaryotic wobble uridine modifications promote a functionally redundant decoding system. *Mol. Cell Biol.*, **28**, 3301–3312.
90. Vendeix,F.A., Murphy,F.V. 4th, Cantara,W.A., Leszczyńska,G., Gustilo,E.M., Sproat,B., Malkiewicz,A. and Agris,P.F. (2012) Human tRNA(Lys3)(UUU) is pre-structured by natural modifications for cognate and wobble codon binding through keto-enol tautomerism. *J. Mol. Biol.*, **416**, 467–485.
91. Lee,J.C. and Gutell,R.R. (2004) Diversity of base-pair conformations and their occurrence in rRNA structure and RNA structural motifs. *J. Mol. Biol.*, **344**, 1225–1249.